JOURNAL OF MODERN OPTICS, 1996, VOL. 43, NO. 12, 2463–2483

Scattering by lacunary gratings

G. GUIDA, G. TAYEB and D. MAYSTRE

Laboratoire d'Optique Electromagnétique, Unité de Recherche Associée au CNRS, No. 843, Faculté des Sciences et Techniques de St Jérôme, Case 262, 13397 Marseille Cedex 20, France

(*Received 25 January 1996; revision received 11 April 1996*)

Abstract. The paper is devoted to a theoretical and numerical study of lacunary gratings, namely, gratings where some lines are missing. From a rigorous electromagnetic theory of scattering by this structure, the limits of validity of three approximate and simple theories are given. These approximate theories are used in order to predict some interesting properties of lacunary gratings. Finally, we try to give a quantitative answer to the following question: how to detect the lacunary defect ratio from intensity measurements?

1. Introduction

The study of phenomena generated by the transition between order and disorder is one of the most fascinating topics of Modern Physics. In the frame of Optics and Electromagnetics, many papers have been devoted to this subject in recent years. Most of these papers are devoted to the phenomena of enhanced backscattering [1–3], and localization of light [4–10].

A continuous transition from order to disorder can be obtained by considering quasi-gratings [11], rough surfaces generated by a random perturbation of a periodic profile [12], etc.

In the present paper, we deal with another example of such structures: the lacunary grating. Such a grating is obtained by removing some rods in a grid-grating. From a practical point of view, grid-gratings can be used for reduction of Radar Cross Section, thanks to their remarkable absorption properties. An application of the study will be the estimation of the mismatch between expected and actual performances of such devices provoked by construction defects.

The numerical results are obtained from a rigorous theory of scattering by a finite number of two-dimensional (2D) cylinders [13]. Comparisons are made between the rigorous numerical data and those derived from simpler but approximate theoretical methods.

2. The rigorous theory in outline

We consider the lacunary grating represented in figure 1. A grating of period d containing a finite number N of rods has been modified by removing N_s rods. These rods are made with a perfectly conducting material or a dielectric of optical index ν (possibly complex). This grid is illuminated by a transverse electric (TE) (s) polarized plane wave with wavelength λ (in vacuum) and incidence angle α. It has been shown in [13] that the field in the vicinity of one rod can be expressed by a

0950–0340/96 $12·00

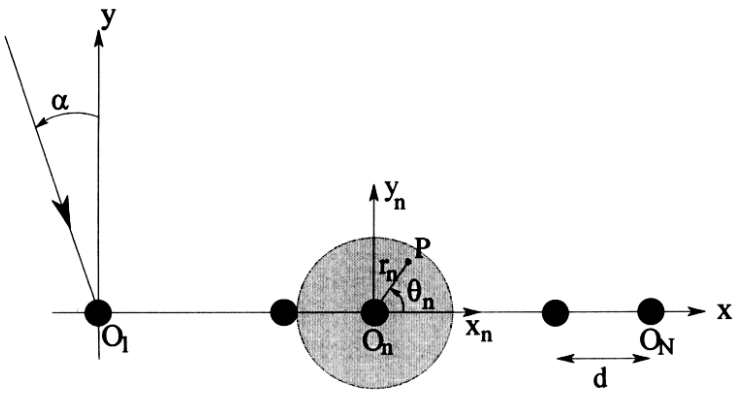

Figure 1. A Lacunary grating with $N = 7$ and $N_s = 2$.

Fourier–Bessel expansion. For instance, for the nth rod, the field at a point P of the greyed homogeneous region of figure 1 can be written in the form of the sum of a local incident field $E_n^i(P)$ and a local diffracted field $E_n^d(P)$:

$$E(P) = E_n^i(P) + E_n^d(P) \tag{1}$$

with

$$E_n^i(P) = \sum_{q=-\infty}^{+\infty} a_{n,q} J_q(kr_n) \exp(iq\theta_n) \tag{2}$$

$$E_n^d(P) = \sum_{q=-\infty}^{+\infty} b_{n,q} H_q^{(1)}(kr_n) \exp(iq\theta_n) \tag{3}$$

where r_n and θ_n are the polar coordinates of P in the system of coordinates x_n, y_n linked with the nth rod, $a_{n,q}$ and $b_{n,q}$ complex coefficients, and $k = 2\pi/\lambda$. It must be emphasized that the local incident field $E_n^i(P)$ is generated not only by the actual incident field $E^i(P)$ given by:

$$E^i(P) = \exp(ik(x \sin\alpha - y \cos\alpha)) \tag{4}$$

but also by the field scattered by the other rods in the direction of the nth rod. At infinity, the field E^d scattered by the entire set of rods can be written in the form:

$$E^d(P) = \sum_{q=-\infty}^{+\infty} b_q H_q^{(1)}(kr) \exp(iq\theta) \tag{5}$$

where r and θ are the polar coordinates of P in the general system of coordinates (x, y) linked with the first rod. From Graf's formula [14], the coefficients b_q can be deduced from the $b_{n,q}$ by:

$$b_q = \sum_{n \in \mathcal{N}} \sum_{p=-\infty}^{+\infty} b_{n,p} J_{q-p}(k(n-1)d) \tag{6}$$

where $\mathcal{N}$ denotes the set of $N_r = N - N_s$ remaining rods. Using the S-matrices S_n of the rods defined by:

$$\forall q, \qquad b_{n,q} = \sum_{p=-\infty}^{+\infty} S_{n,q,p} a_{n,p} \tag{7}$$

and Graf's formula, then by truncating the set of coefficients $a_{n,q}$ and $b_{n,q}$ from $q = -Q$ to $+Q$, it has been shown in [13] that the coefficients $a_{n,q}$ and $b_{n,q}$ satisfy a square linear system of $N_r(2Q+1)$ equations.

From the asymptotic expression of the Hankel function, the scattered field given by (5) can be written at infinity in the form:

$$E^d(P) = g(\theta)\frac{\exp(ikr)}{r^{1/2}} \tag{8}$$

with

$$g(\theta) = \left(\frac{2}{\pi k}\right)^{1/2} \exp\left(-i\frac{\pi}{4}\right) \sum_{q=-Q}^{+Q} (-i)^q b_q \exp(iq\theta) \tag{9}$$

The intensity at infinity (or bistatic differential cross-section) is defined by:

$$D(\theta) = 2\pi|g(\theta)|^2 \tag{10}$$

and for lossless cylinders the energy balance criterion can be written in the form:

$$\int_0^{2\pi} |g(\theta)|^2 \, d\theta + 2\lambda^{1/2} \operatorname{Re}\left[\exp\left(i\frac{\pi}{4}\right) g\left(\alpha - \frac{\pi}{2}\right)\right] = 0 \tag{11}$$

The use of this formalism needs the calculation of the S-matrices of the rods, thus the calculation of the scattering properties of each rod. It is fundamental to notice that the S-matrix is an intrinsic notion, and is not modified by the existence of the other rods. Of course, if all the rods are identical, only one S-matrix has to be determined. When the shape of the rods is circular, the calculation of the S-matrix is analytic and this matrix reduces to its diagonal. For rods of arbitrary shapes, a boundary finite-elements method is used. The reader can find in [13] various tests of validity of the results.

3. Approximate methods

When the size of the rods is small compared with the wavelength, it has been shown in [13] that the expressions of the scattered and incident fields E_n^d and E_n^i, given by equations (2) and (3), reduce to the isotropic term corresponding to $q = 0$:

$$E_n^i(P) = a_{n,0} J_0(kr_n) \tag{12}$$

$$E_n^d(P) = b_{n,0} H_0^{(1)}(kr_n) \tag{13}$$

Thus, according to (7), the scattering matrix reduces to its central coefficient:

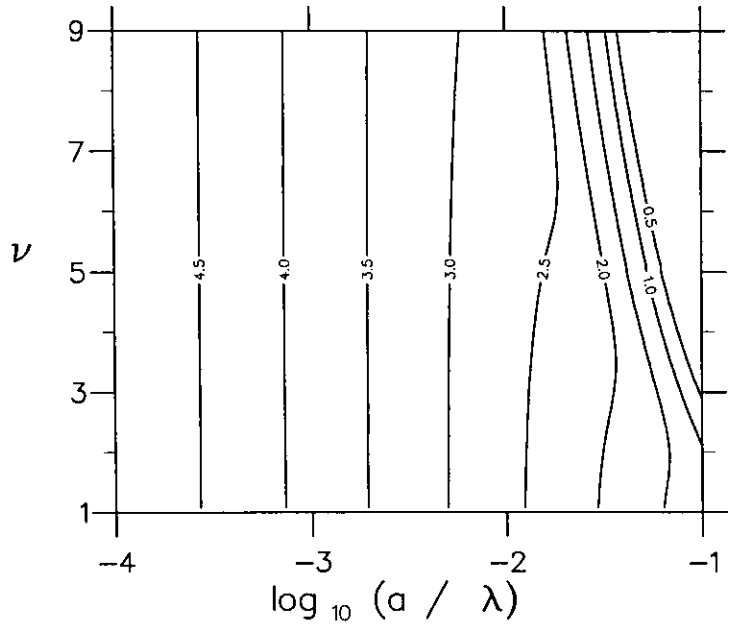

Figure 2. Isolines of $\mathcal{J}$ for dielectric rods of radius a and index ν.

$$b_{n,0} = S_{n,0,0}a_{n,0} \tag{14}$$

Note that here, the word 'isotropic' is used in order to state that the scattered field does not depend on the scattering direction.

In order to specify the domain of validity of this isotropic approximation, we have drawn in figure 2 a graph showing the isolines of

$$\mathcal{J} = \log_{10}\left|\frac{b_{1,0}H_0^{(1)}(ka)}{b_{1,1}H_1^{(1)}(ka)}\right| \tag{15}$$

when the set of rods reduces to only one ($N = 1$), a being the radius of the rod. This quantity is the ratio of the fundamental (isotropic term) to the first harmonic (anisotropic term) of the scattered field given by (3), thus it expresses the degree of isotropy of the scattered field at the boundary of the rod. Note that $|H_0^{(1)}(x)/H_1^{(1)}(x)|$ is a monotonic increasing function of x. As a consequence, $\mathcal{J}$ represents the smallest value of this ratio in the region $x \geq a$ outside the rod, where the scattered field is defined. In other words, $\mathcal{J}$ is the most pessimistic estimate of the isotropy outside the rod. In figure 2, the index ν of the rods is assumed to be real. This figure fully confirms the fact that the anisotropy increases as a/λ is increasing. When a/λ is smaller than 10^{-2}, $\mathcal{J}$ becomes linearly dependent on $\log_{10}(a/\lambda)$, and independent of ν. The influence of ν is restricted to values of a/λ greater than 10^{-2}. Roughly speaking, the anisotropy increases with the index of the rods.

In figure 3, we are dealing with the case where the rods have a conductivity σ, the relative permittivity being given by:

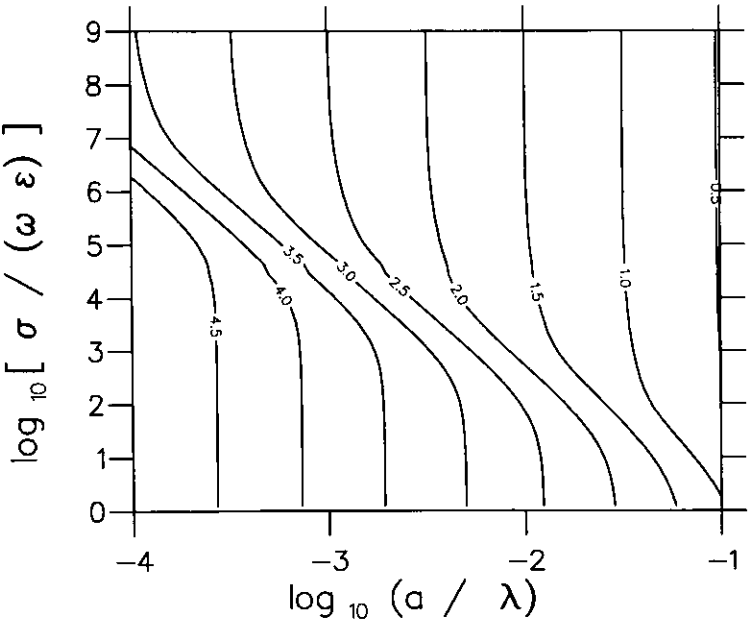

Figure 3. Isolines of $\mathscr{J}$ for ohmic rods of radius a and conductivity σ.

$$\epsilon = 1 + \mathrm{i}\frac{\sigma}{\epsilon_0 \omega} \tag{16}$$

ω being the pulsatance. The variation of the ordinate from 0 to 9 has been chosen in order to match with the entire range of σ/ω from ultraviolet to microwave regions. The first conclusion that emerges is the existence of two asymptotic limits of the isolines, on both sides of the range of σ/ω. For small values of the ordinate, the limit of $\mathscr{J}$ is the same as in figure 2. However, it must be noted that the range of variation of the modulus of the index is much smaller in figure 2 than in figure 3. As regards the vertical asymptotic behaviour of the isolines for large values of the conductivity, one must remark that for a given value of the radius, the metallic rod tends to a perfectly conducting one when σ tends to infinity. Using figures 2 and 3, one can appreciate, in a given problem of scattering by dielectric or metallic rods, whether a model neglecting the anisotropy of the scattered field is acceptable or not. For instance, if the desired accuracy on the field is equal to 10^{-2}, the isotropic approximation can be used at the left of the isoline $\mathscr{J} = 2$.

Now, let us come back to the problem of the lacunary grating defined in section 2. When the size of the rods is small, it must be noted that the coefficient $a_{n,0}$ of the incident field in (12) is nothing but the value of the local incident field at O_n. This field at O_n can be calculated in another way by remembering that the local incident field at O_n is the sum of the actual incident field $E^{\mathrm{i}}(O_n)$ and the field scattered by the other rods:

$$a_{n,0} = E^{\mathrm{i}}(O_n) + \sum_{\substack{m \in \mathcal{N} \\ m \neq n}} b_{m,0} H_0^{(1)}(kd|n-m|) \tag{17}$$

with, according to (4),

$$E^{\mathrm{i}}(O_n) = \exp(\mathrm{i}k(n-1)d\sin\alpha) \tag{18}$$

Since the coefficients $b_{m,0}$ tend to zero when the size of the rods decreases, it can be assumed, as a first approximation, that the sum contained in the right-hand member of (17) can be neglected. With this approximation, and using (14), the coefficients $b_{n,0}$ are given by:

$$b_{n,0} = S_{n,0,0} \exp(\mathrm{i}k(n-1)d \sin\alpha) \tag{19}$$

The coefficients of the field at infinity given by (6) become:

$$b_q = \sum_{n \in \mathcal{N}} S_{n,0,0} \exp(\mathrm{i}k(n-1)d \sin\alpha) J_q(k(n-1)d) \tag{20}$$

and from (9), the complex amplitude $g(\theta)$ can be written in the form:

$$g(\theta) = \left(\frac{2}{\pi k}\right)^{1/2} \exp\left(-\mathrm{i}\frac{\pi}{4}\right) \sum_{n \in \mathcal{N}} S_{n,0,0} \exp[\mathrm{i}(n-1)kd(\sin\alpha - \cos\theta)] \tag{21}$$

When all the rods are identical, let us write $S_{n,0,0} = S_{0,0}$, and thus:

$$g(\theta) = \left(\frac{2}{\pi k}\right)^{1/2} \exp\left(-\mathrm{i}\frac{\pi}{4}\right) S_{0,0} \sum_{n \in \mathcal{N}} \exp[\mathrm{i}(n-1)kd(\sin\alpha - \cos\theta)] \tag{22}$$

If $N_s = 0$, the summation in the right-hand member of (20) extends to all the values of n from 1 to N, thus:

$$g(\theta) = \left(\frac{2}{\pi k}\right)^{1/2} \exp\left(-\mathrm{i}\frac{\pi}{4}\right) S_{0,0} \exp\left[\mathrm{i}\left(\frac{N-1}{2}\right)kd(\sin\alpha - \cos\theta)\right] \times \frac{\sin((N/2)kd(\sin\alpha - \cos\theta))}{\sin((kd/2)(\sin\alpha - \cos\theta))} \tag{23}$$

Denoting by $g_1(\theta)$ the amplitude scattered at infinity by the first rod:

$$g_1(\theta) = \left(\frac{2}{\pi k}\right)^{1/2} S_{0,0} \exp\left(-\mathrm{i}\frac{\pi}{4}\right) \tag{24}$$

and defining:

$$\varphi = kd(\sin\alpha - \cos\theta) \tag{25}$$

(23) can be written in the form:

$$g(\theta) = g_1(\theta) \exp\left(\mathrm{i}\left(\frac{N-1}{2}\right)\varphi\right) \frac{\sin(N\varphi/2)}{\sin(\varphi/2)} \tag{26}$$

and we deduce the intensity at infinity:

$$D(\theta) = D_1 \left| \frac{\sin(N\varphi/2)}{\sin(\varphi/2)} \right|^2 \tag{27}$$

D_1 being the isotropic intensity scattered at infinity by the first rod. The expression of the intensity has the same shape as that given in the Physical Optics approximation [15]. It can be noted that the maximum values of $D(\theta)$ are obtained when $\varphi = 2\pi l$ (l integer). This remark allows one to determine the direction of grating orders.

If some rods are removed, the field scattered at infinity by the lacunary grating can be obtained by summing the entire sum ($n \in [1, N]$) in (22) then by removing the exponentials corresponding to the N_s rods:

$$g(\theta) = g_1(\theta) \left[\exp\left(i\left(\frac{N-1}{2}\right)\varphi \right) \frac{\sin(N\varphi/2)}{\sin(\varphi/2)} - \sum_{\substack{n \in [1,N] \\ n \notin \mathcal{N}}} \exp(i(n-1)\varphi) \right] \tag{28}$$

This first approximate theory does not take into account either the anisotropy of the field scattered by one rod, or the coupling between the rods. Figures 2 and 3 permit one to evaluate the domain of validity of the isotropic model. On the other hand, the interaction between rods is a more complicated phenomenon classically termed 'multiscattering'. It is possible to improve the previous approximate theory by including the multiscattering phenomenon to first order. With this aim, we can include the sum of (17) in equation (14). The new approximation $\tilde{b}_{n,0}$ will be deduced by the first approximation $b_{n,0}$ given by (19) from:

$$\tilde{b}_{n,0} = S_{n,0,0} \left[E^i(O_n) + \sum_{\substack{m \in \mathcal{N} \\ m \neq n}} b_{m,0} H_0^{(1)}(kd|n-m|) \right] \tag{29}$$

The field at infinity can be obtained from (6), (8), (9) and (10). The interest of this second approximate theory lies in its simplicity. Even though it is not possible to express the field at infinity in closed form, this theory can be easily implemented on a small computer.

4. Validity of the approximate methods

In order to know the domain of validity of the approximate theories, we have compared their predictions with the results provided by the rigorous theory [13]. The precision of these approximate theories has been compared by using, for each of them, the following criterion:

$$\Delta = \frac{\int |g_a(\theta) - g_r(\theta)|^2 \, d\theta}{\int |g_r(\theta)|^2 \, d\theta} \tag{30}$$

where $g_a(\theta)$ and $g_r(\theta)$ denote the approximate and rigorous values of the scattered amplitude at infinity. Since obviously the coupling and the anisotropy phenomena do not depend on N_s (at least if N_s is small) we have chosen, for simplicity, to consider the case $N_s = 0$.

Figure 4 shows the value of Δ versus $\log_{10}(a/\lambda)$, for a grating made with

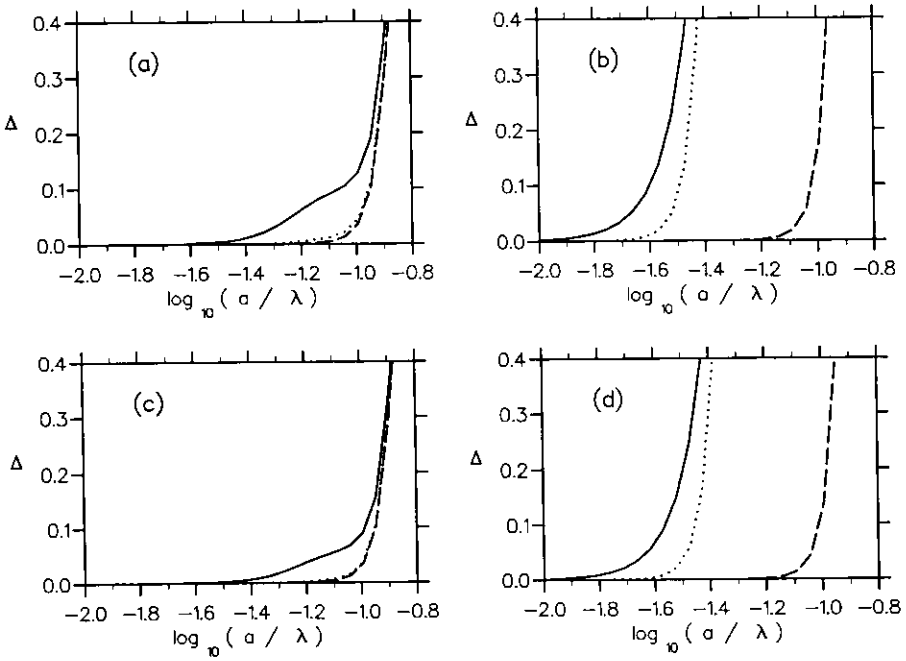

Figure 4. Discrepancy factor Δ versus $\log_{10}(a/\lambda)$ for (*a*) $d/\lambda = 1{\cdot}5$, (*b*) $d/\lambda = 2$, (*c*) $d/\lambda = 2{\cdot}5$ and (*d*) $d/\lambda = 3$. The number of rods is $N = 30$, the index of the rods $\nu = 2{\cdot}5$, the incidence $\alpha = 0°$. Solid line: first approximate method; dotted line: second approximate method; dashed line: third approximate method.

circular rods of radius a, and for various values of d/λ. The discrepancy factor Δ has been drawn for the first, second and third approximate methods, the last one being derived from the rigorous theory [13] by limiting the Fourier–Bessel expansion of the field to the central (isotropic) term. Thus, all these approximate methods neglect the anisotropy of the field. The first one also neglects the multiscattering phenomena between rods, the second one takes into account these multiscattering phenomena at the first order while the third one takes all the multiscattering phenomena into account. The most striking feature of figure 4 is the big difference between the curves at the left-hand side (4 (*a*) and 4 (*c*)) and the curves at the right-hand side (4 (*b*) and 4 (*d*)). The discrepancy is much larger in 4 (*b*) and 4 (*d*) where the ratio d/λ is an integer, except for the third theory. This result is not surprising. Indeed, since we are at normal incidence, the grating generates orders in the direction $\theta = 0°$ and $\theta = 180°$, thus the multiscattering phenomena are strongly enhanced. As a consequence, the first and second theories become rapidly ineffective as a/λ is increased, the second theory being always much better than the first one. On the other hand, in figures 4 (*a*) and 4 (*c*), the second theory provides a discrepancy factor very close to that of the third theory, and much better than that of the first theory. In figures 4 (*a*) and 4 (*c*), the limit of validity of the first theory ($\Delta < 0{\cdot}05$) is close to $-1{\cdot}25$ ($a/\lambda \approx 0{\cdot}06$) and the limit of the other theories is close to -1 ($a/\lambda \approx 0{\cdot}10$). On the other hand, in figures 4 (*b*) and 4 (*d*) the respective limits of validity of the first and second theories are close to $-1{\cdot}6$ ($a/\lambda \approx 0{\cdot}025$) and $-1{\cdot}5$ ($a/\lambda \approx 0{\cdot}032$). Most of these results can be predicted from figure 2, where it appears that instead of the limit of validity of the isotropic

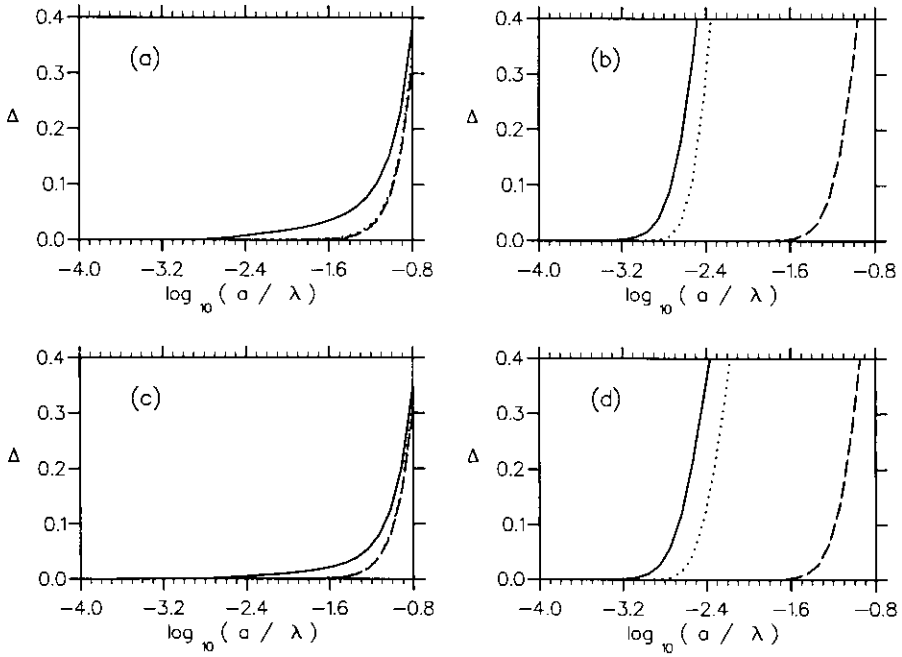

Figure 5. Same as figure 4, but for conducting rods of conductivity $\sigma = 750\,\Omega^{-1}\,m^{-1}$ and $\lambda = 30\,mm$ (i.e. $\log_{10}(\sigma/\omega\epsilon_0) = 3{\cdot}13$).

model (isoline 1·0 for $\nu = 2{\cdot}5$) is slightly larger than $\log_{10}(\lambda/a) = 1$. Thus the third theory must provide precise results until this limit. On the other hand, the first and second theories cannot provide a sufficiently precise approximation of the multi-scattering phenomena inside the range of validity of the isotropic model. In conclusion, due to its simplicity and its superiority on the first one, the second theory is a good choice, provided we are far from the condition of passing-off of one order (Rayleigh anomaly).

Figure 5 shows the results of the equivalent study for lossy materials. The conductivity $\sigma = 750\,\Omega^{-1}\,m^{-1}$ is that of new materials in the microwave region [13], obtained by homogenization process in order to absorb radar radiation. As for lossless materials, the limit of validity of the isotropic model can be deduced from our prior study (figure 3). Since $\log_{10}(\sigma/\omega\epsilon_0) = 3{\cdot}13$, the figure 3 shows that the limit of the isotropic model (isoline 1·0) is close to $\log_{10}(a/\lambda) = -1{\cdot}5$, which is approximately the limit of the third theory in figure 5. When no passing-off occurs (left side of figure 5), the limit of the second approximate theory is almost identical while the limit of the first theory is much lower. On the other hand, at the passing-off (right side of figure 5), the limit of the first and second approximate theories are close to $\log_{10}(a/\lambda) = -2{\cdot}7$, which corresponds to a radius of the rod equal to $0{\cdot}002\,\lambda$. Thus the conclusion of figure 5 is close to that of figure 4, but with lower limits of validity of all the approximate theories.

Figures 4 and 5 have shown the vital importance of d/λ on the error, due to multiscattering effects. Figure 6 shows, for $\log_{10}(a/\lambda) = -1{\cdot}2$, the error Δ versus d/λ, for normal incidence. This figure fully confirms what appeared in figures 4 and 5: the passing-off of grating orders drastically increases the multiscattering. The simplest approximate theory generates an error always greater than 5%. The

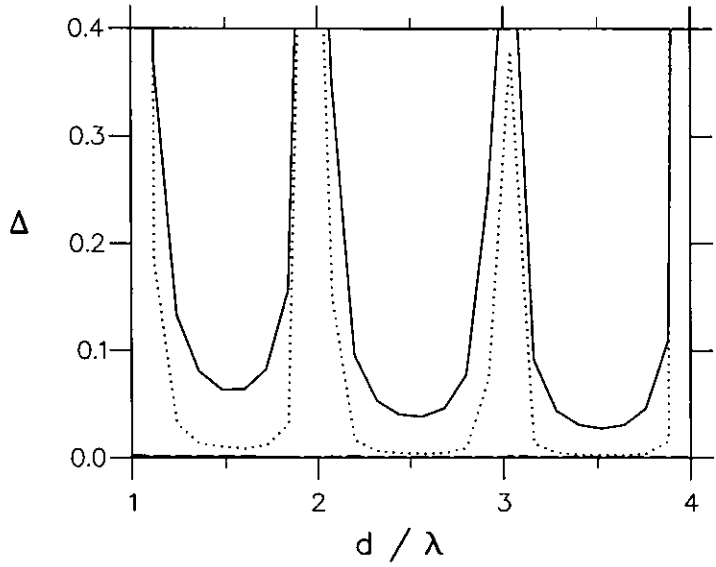

Figure 6. Same as figure 4, but the abscissa is d/λ, and for $\log_{10}(a/\lambda) = -1{\cdot}2$. The dashed line given by the third method is very close to the abscissa axis.

second theory provides much better results far from the passing-off. The third approximate theory provides good accuracy over the entire range of d/λ.

5. Numerical results

5.1. *Prediction coming from the first approximate theory*

Thanks to its simplicity, the first approximate theory allows one to conjecture very simple properties of lacunary gratings, at least in its domain of validity. First, let us consider the intensity scattered in the directions of the grating orders, where $\varphi = 2\pi l$ (l is an integer). In that case, equation (28) shows that:

$$g(\theta) = (N - N_s)g_1(\theta) \tag{31}$$

Thus, the result is quite simple: the scattered amplitude at infinity in the directions of the grating orders is proportional to the number of rods in the lacunary grating, regardless of the location of the rods. Since, in this approximation, $g_1(\theta)$ is independent of θ, all these scattered amplitudes are equal. In figure 7, the rigorous theory has been used in order to draw, for a lacunary grating, the modulus of the normalized scattered field $g_N(\theta)$ at infinity, defined by:

$$g_N(\theta) = \frac{g(\theta)}{N - N_s} \tag{32}$$

According to (31), $g_N(\theta)$ must identify with the field $g_1(\theta)$ scattered by a single rod in the directions of grating orders. When the radius of the rods is small (figure 7 (*a*)), we are in the range of validity of the first approximation (see figure 4) and our prediction is confirmed by rigorous results. On the other hand, for a greater value of the radius (figure 7 (*b*)), this prediction fails.

The first approximation allows us to deduce a second property: the rule of

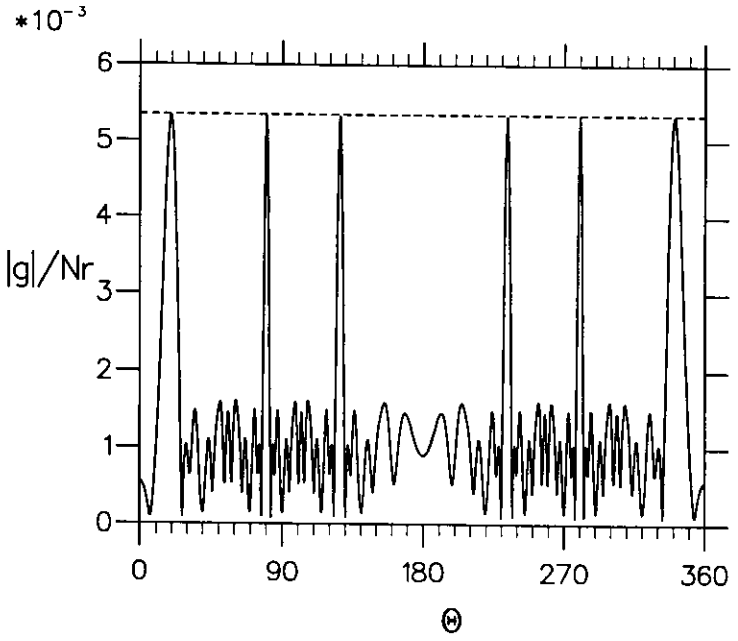

(*a*)

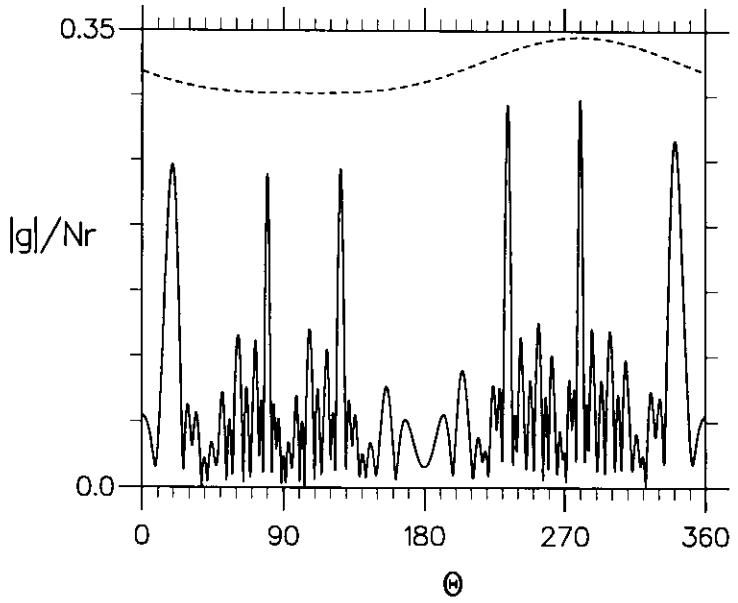

(*b*)

Figure 7. (*a*) Solid line: modulus of $g_N(\theta)$ versus θ for a lacunary grating: $N = 15$, $N_s = 4$ (the suppressed rods are rods number 2, 5, 10 and 12), $a = 0{\cdot}01$, $\nu = 2{\cdot}5$, $d = 1{\cdot}3$, $\lambda = 1$, $\alpha = 10°$. Dashed line: modulus of the field scattered by a single rod $g_1(\theta)$. (*b*) Same as (*a*), but for $a = 0{\cdot}1$.

equivalence between two complementary lacunary gratings. Starting from the finite grating A (N equidistant rods), let us consider two lacunary gratings (B and C): the lacunary grating B is obtained from A by removing N_s rods, and the complementary lacunary grating C is obtained from A by removing the $N - N_s$ rods of B. Let us denote by $g_A(\theta)$, $g_B(\theta)$ and $g_C(\theta)$ the amplitudes scattered at infinity by A, B and C. A straightforward consequence of (22) is, for any value of θ:

$$g_B(\theta) + g_C(\theta) = g_A(\theta) \tag{33}$$

Figure 8 (*a*), drawn from the rigorous theory, shows the validity of this conjecture when the radius of the rods is small. The modulus of the two members of (33) are very close to each other, in such a way that the curves look identical. In contrast, for a larger radius of the rods (Figure 8 (*b*)), the coupling between the rods is not negligible and the curves differ significantly.

Moreover, if N is large, the field scattered by the finite grating A is concentrated at the vicinity of the grating orders; as a consequence, the fields scattered by the two complementary gratings B and C are opposite outside these directions, thus the intensities are equal and the gratings are equivalent. Figure 9, also drawn from the rigorous theory, shows the validity of this prediction for a grating having a large number of rods.

5.2. *Influence of the lacunary defect ratio on the scattered field at infinity*

Our aim in this section is to evaluate the influence of the lacunary defect ratio τ:

$$\tau = N_s/N \tag{34}$$

on the scattered amplitude at infinity. For small values of N_s, the behaviour of a lacunary grating should not differ strongly from that of a perfect finite grating. On the other hand, when the lacunary defect ratio approaches unity, the lacunary grating is quite different from the finite grating and one can predict that the scattered field has lost all information on the period of the initial grating. Thus, the question that arises is to know what is the transition point, or in other words what is the threshold value of N_s/N up to which the field scattered at infinity by a lacunary grating still contains information on its initial periodic nature. Conversely, another interesting question is to know how to detect efficiently the lacunary defect when N_s/N is small.

In order to answer these questions, it is necessary to specify first what are the available characteristics of the scattered field at infinity: intensity or both intensity and phase. In order to evaluate the relative importance of these data, we are led to define two criteria, expressed in the form:

$$DI = \left(\frac{\int_0^{2\pi} \left| |g(\theta)|^2 - |g_l(\theta)|^2 \right| \mathrm{d}\theta}{\int_0^{2\pi} \left| |g(\theta)|^2 + |g_l(\theta)|^2 \right| \mathrm{d}\theta} \right)^{1/2} \tag{35}$$

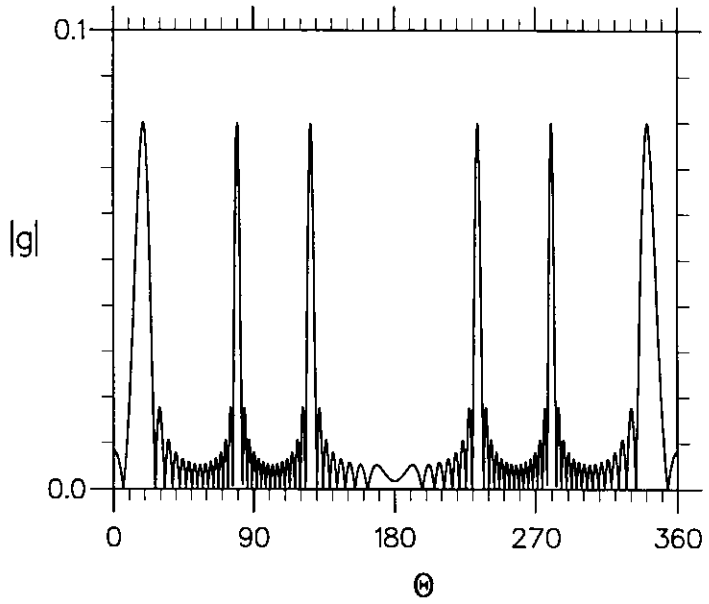

(*a*)

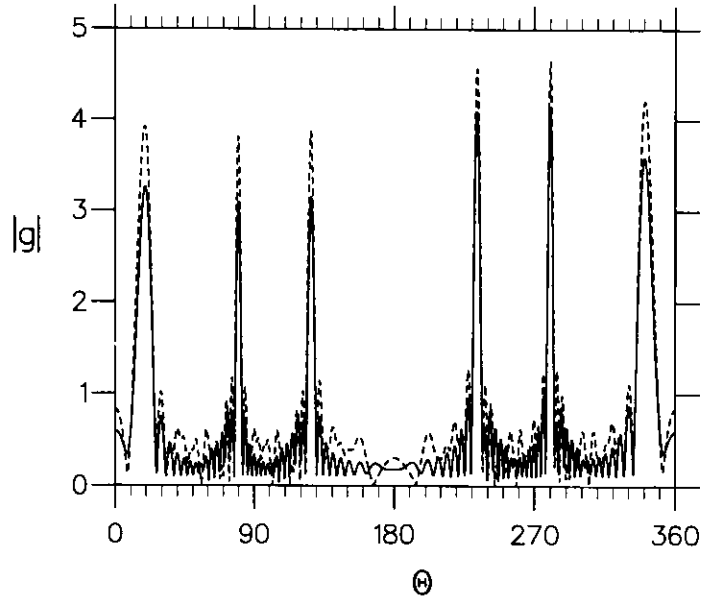

(*b*)

Figure 8. (*a*) For the same lacunary grating B as in figure 7 (*a*). Solid line: modulus of $g_A(\theta)$. Dashed line: modulus of $g_B(\theta) + g_C(\theta)$. The two curves look identical. (*b*) Same as (*a*), but for $a = 0{\cdot}1$.

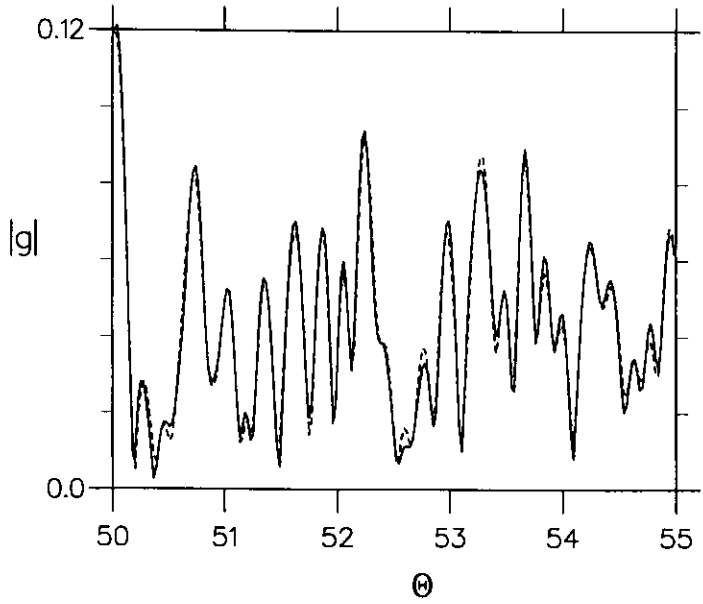

Figure 9. Solid line: modulus of $g_B(\theta)$ versus θ for a large lacunary grating in a region where no diffraction order exists: $N = 400$, $N_s = 100$, $a = 0{\cdot}01$, $\nu = 2{\cdot}5$, $d = 1{\cdot}3$, $\lambda = 1$, $\alpha = 10°$. Dashed line: modulus of $g_C(\theta)$ for the complementary grating ($N_s = 300$).

$$DA = \left(\frac{\int_0^{2\pi} |g(\theta) - g_l(\theta)|^2 \, d\theta}{\int_0^{2\pi} |g(\theta) + g_l(\theta)|^2 \, d\theta} \right)^{1/2} \tag{36}$$

where $g(\theta)$ and $g_l(\theta)$ are respectively the complex amplitudes scattered at infinity by the perfect and lacunary gratings. In the following, all these functions will be computed using the code based on the rigorous theory described in section 2. Of course, the calculation of DA needs the knowledge of the argument of the field at infinity while DI can be deduced from intensity measurements. Further, equation (32) leads us to introduce two supplementary criteria:

$$DI_N = \left(\frac{\int_0^{2\pi} \left| \left| \frac{g(\theta)}{N} \right|^2 - \left| \frac{g_l(\theta)}{N - N_s} \right|^2 \right| d\theta}{\int_0^{2\pi} \left| \left| \frac{g(\theta)}{N} \right|^2 + \left| \frac{g_l(\theta)}{N - N_s} \right|^2 \right| d\theta} \right)^{1/2} \tag{37}$$

$$DA_N = \left(\frac{\int_0^{2\pi} \left| \frac{g(\theta)}{N} - \frac{g_l(\theta)}{N - N_s} \right|^2 d\theta}{\int_0^{2\pi} \left| \frac{g(\theta)}{N} + \frac{g_l(\theta)}{N - N_s} \right|^2 d\theta} \right)^{1/2} \tag{38}$$

These criteria take into account the behaviour of the amplitude of the field in the diffracted orders. Figure 10 shows the results obtained by starting from a grating having 30 rods. The first conclusion which arises is the regularity of the behaviour of the lacunary grating when τ is increased except at the origin. It is noteworthy that the four curves look very similar, even when the size of the rods is increased. However, DI is always greater than the other criteria. In other words, if the intensity scattered by the perfect finite grating is available, it appears that a good criterion to detect the lacunarity is DI, i.e. a comparison between the intensities. Furthermore, it appears that the normalization of the field with respect to the number $N - N_s$ of rods is not worthwhile. Bearing in mind (32), this remark can be surprising for small rods. In fact, this remark shows that the contribution to DI_N and DA_N of the field scattered between the direction of the grating orders plays a vital role.

The main drawback of the criteria used in the previous paragraph lies in the fact that they require the knowledge of the field scattered at infinity by the perfect finite grating associated with the lacunary grating. Moreover, figure 10 leads us to separate the direction of the grating orders from the other ones. Thus we have defined the incoherence factor ξ by:

$$\xi = \frac{\left\langle \int_{\text{ext}} |g_l(\theta)|^2 \, \mathrm{d}\theta \right\rangle}{\left\langle \int_0^{2\pi} |g_l(\theta)|^2 \, \mathrm{d}\theta \right\rangle} \stackrel{\text{def}}{=} \frac{\langle J_{\text{ext}} \rangle}{\langle J_{\text{tot}} \rangle} \tag{39}$$

where J_{ext} is the integral of the intensity outside the central peaks of intensity of the diffracted orders (the central peak of a given order being defined as the interval between the two minima of intensity located on both sides of the direction predicted by the grating formula), J_{tot} the total integrated intensity, and the brackets denote the average value on a large number of random realizations of the lacunary grating. It can be expected that this criterion will provide direct information on τ. Indeed, if τ tends to zero, the main part of the intensity goes to the diffraction order and thus ξ should be close to 0. On the other hand, when τ is increased, the peaks in the diffracted orders tend to disappear and thus ξ should tend to 1. If the behaviour of ξ between these two limits is not too sensitive to the various parameters of the grating, the knowledge of ξ will give directly the lacunary defect factor τ.

Figure 11 shows the incoherence factor versus τ. The most interesting features of the curves lie in the fact that the curves are close to straight lines having the same ordinate ξ_0 at the origin ($\xi_0 \approx 0{\cdot}1$) and very close slopes. The value of ξ_0 can be easily calculated using the first approximation of section 3. Indeed, if τ is equal to 0, equation (27) shows that the intensity tends to 0 outside a small range of diffracted angles close to the direction of the grating orders. When N tends to infinity, this range tends to 0. Figure 12 shows the value of $D(\theta)/D_1$ given by equation (27), assuming that $\sin^2(\varphi/2)$ can be replaced by $\varphi^2/4$. It is worth noting that the summit of the pth peak (p beginning at 0 for the central peak) is equal to $4N^2/(2p+1)^2\pi^2$, except for the central peak where the maximum is equal to N^2. As a consequence, taking into account the width of the peaks, the integral of the intensity in the pth peak behaves approximately like $N/(2p+1)^2$.

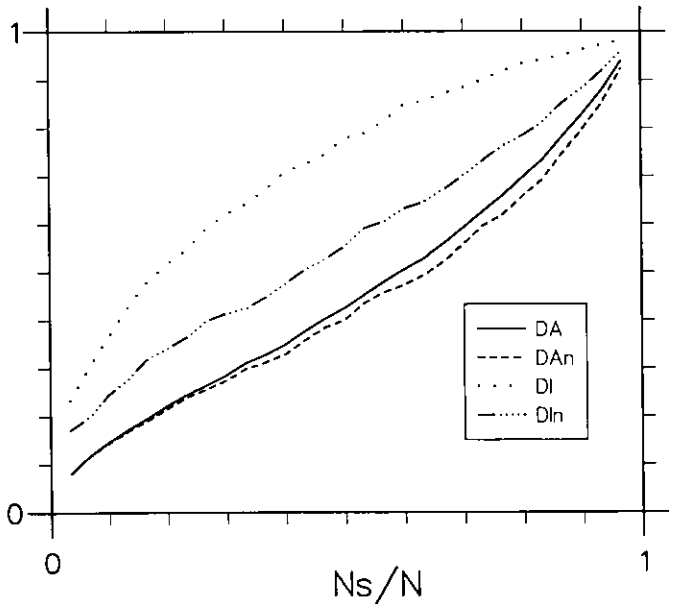

(*a*)

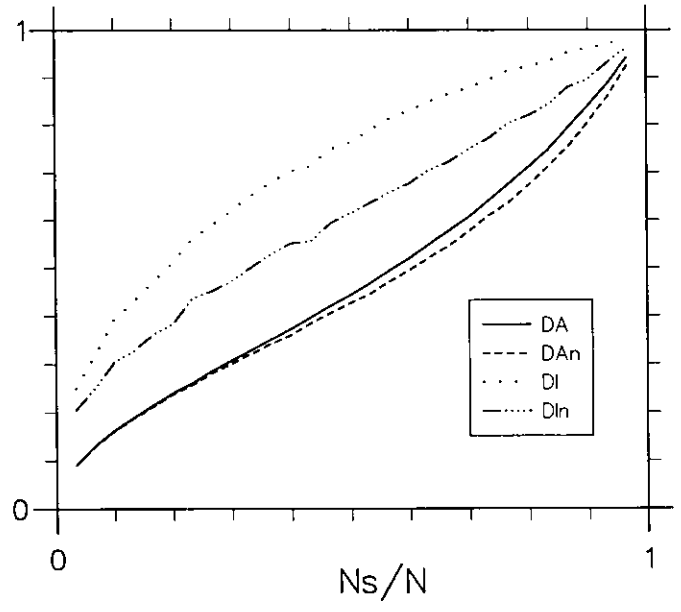

(*b*)

Figure 10. Influence of the lacunary defect ratio on the mismatch with perfect finite grating. The number N of rods is equal to 30 and the other parameters are the same as in figure 9. (*a*) Small rods ($a = 0{\cdot}01$). (*b*) Large rods ($a = 0{\cdot}4$). The results are obtained by taking average values on 10 random realizations of the lacunary grating.

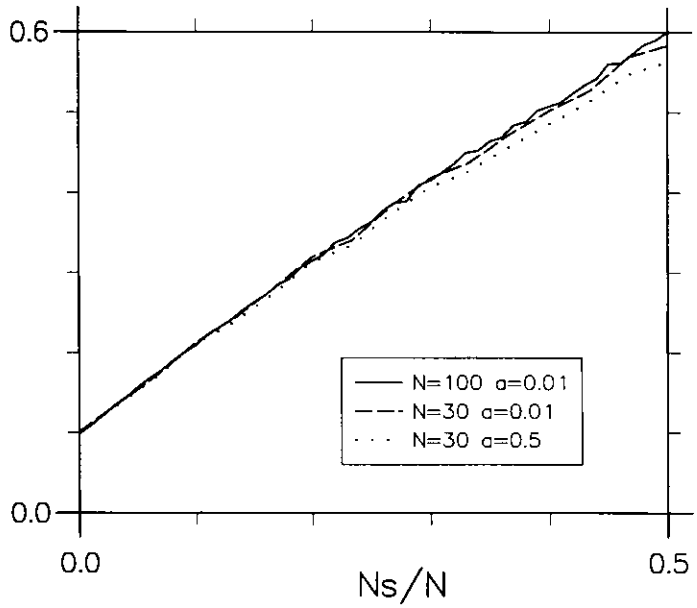

Figure 11. Influence of the lacunary defect on the incoherence factor ξ. The solid line shows the results obtained starting from a grating having 100 rods of index $\nu = 1{\cdot}5$ and radius $a = 0{\cdot}01$, the groove period is $d = 1{\cdot}5$, the wavelength $\lambda = 1$, the incidence $\alpha = 0°$, the average value being made on 100 random realizations. The dashed line shows the same result, but starting from a grating having 30 rods, and the dotted line is for large rods ($a = 0{\cdot}5$).

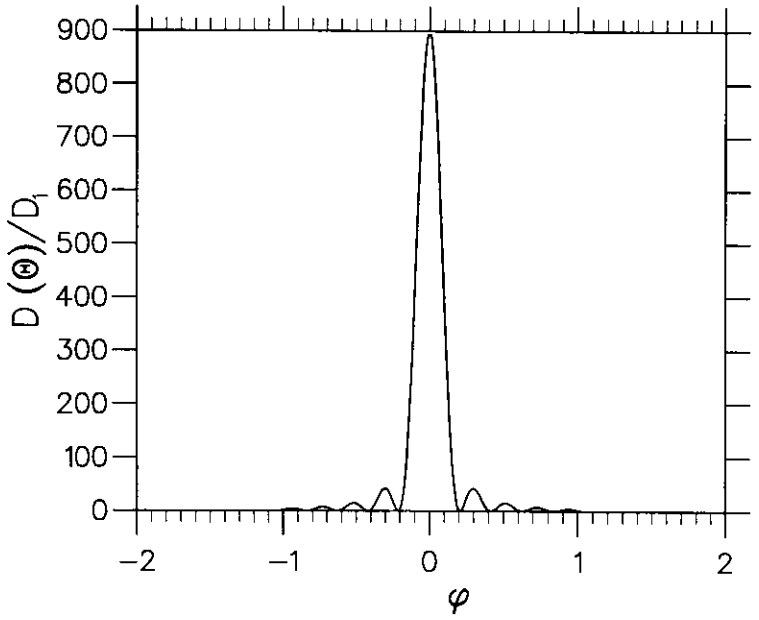

Figure 12. Value of $D(\theta)/D_1$ given by equation (27) assuming that $\sin^2(\varphi/2)$ can be replaced by $\varphi^2/4 (N = 30)$.

In order to calculate the limits of the intensities in the peaks as $N \to \infty$, we define:

$$\eta_p = \int_{2\pi p/N}^{2\pi(p+1)/N} \frac{\sin^2(N\varphi/2)}{\sin^2(\varphi/2)} \left|\frac{d\theta}{d\varphi}\right| d\varphi \tag{40}$$

It is important to notice that η_p is equal to the area of the pth peak except for $p = 0$, η_0 representing half of the area of the central peak. Remarking that when $N \to \infty$, $d\theta/d\varphi$ tends to a constant and $\sin(\varphi/2) \approx \varphi/2$, η_p becomes:

$$\eta_p = 4\frac{d\theta}{d\varphi}\int_{2\pi p/N}^{2\pi(p+1)/N} \frac{\sin^2(N\varphi/2)}{\varphi^2} d\varphi \tag{41}$$

and using the new variable $u = N\varphi/2$, (41) yields:

$$\eta_p = 2N\frac{d\theta}{d\varphi}\int_{\pi p}^{\pi(p+1)} \left(\frac{\sin u}{u}\right)^2 du \tag{42}$$

Finally, if we limit ourselves to the intensity around a given diffraction order,

$$\xi_0 = \frac{\sum_{p=1}^{\infty} \eta_p}{\sum_{p=0}^{\infty} \eta_p} \tag{43}$$

From a mathematical point of view, the approximation made to deduce (41) from (40) requires p to remain finite as N tends to infinity. However (43) is quite correct since the sum converges very rapidly (in $1/p^2$). For example, a straightforward numerical calculation shows that $\eta_1/\eta_0 = 0{\cdot}0521$, $\eta_{10}/\eta_0 = 0{\cdot}0010$ and $\eta_{100}/\eta_0 = 10^{-5}$. Since the value of ξ given by (43) does not depend on the diffracted order, it can be deduced that the same formula holds for the actual value of ξ defined by (39). This theoretical value is:

$$\xi_0 = 0{\cdot}097 \tag{44}$$

Figure 11 shows the validity of this prediction. It is very important to note that this value of the ordinate seems independent of the radius of the rods, even though our prediction was based on an approximation valid for small rods only. Figure 13 gives the corresponding curves for lossy rods. Obviously the conclusion remains the same.

In conclusion, the incoherence factor ξ is very interesting since it can provide for an experimenter a direct estimation of the lacunary defect τ. Of course, a thorough numerical investigation would be necessary to estimate the variation of the slope of $\xi(\tau)$ around the origin; however the present calculation can be considered as very promising.

Finally, in order to conclude this section, an answer will be given to the question asked at the beginning of the section: what is the threshold value of N_s/N up to which the field scattered at infinity by a lacunary grating still contains information on its initial periodic nature? Figure 14 shows the surprising

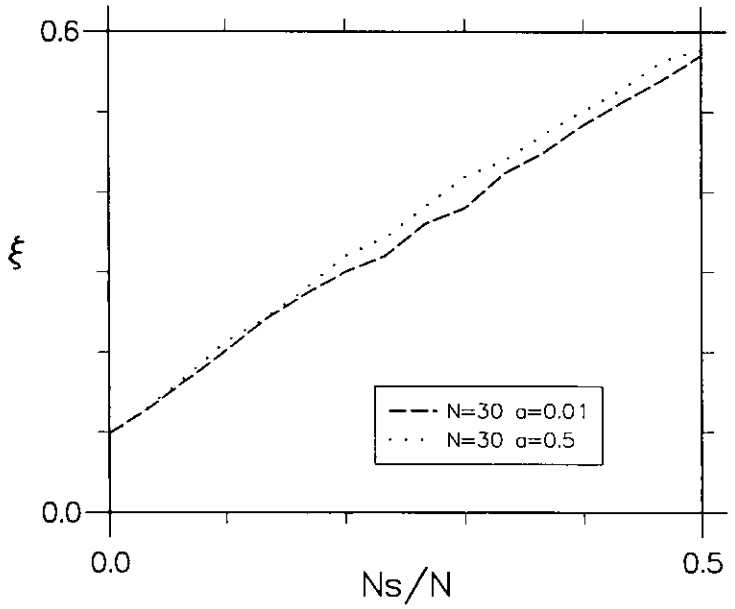

Figure 13. Same as figure 11 but for ohmic rods of conductivity $\sigma = 750\,\Omega^{-1}\,m^{-1}$ and $\lambda = 30$ mm. Dotted line: $a = 0{\cdot}01\lambda$. Dashed line: $a = 0{\cdot}5\lambda$.

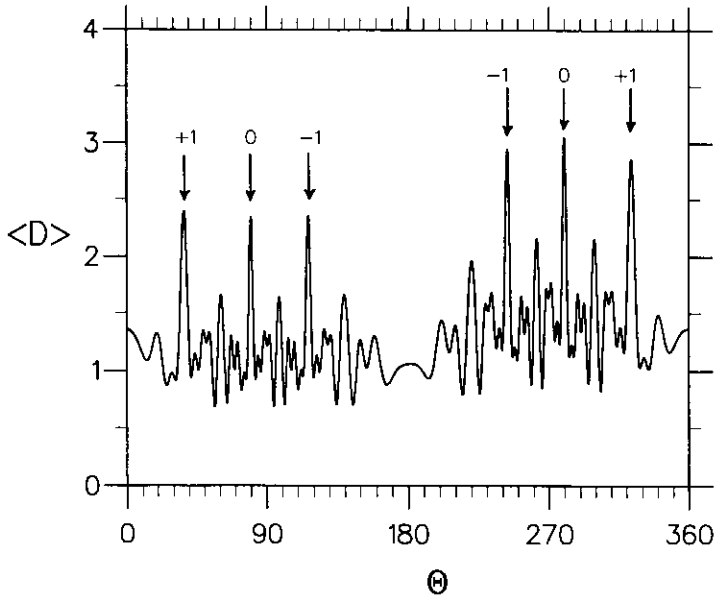

Figure 14. Average value of intensity on 10 random realizations of a lacunary grating with $N = 15$, $N_s = 13$, $a = 0{\cdot}1\lambda$, $d = 1{\cdot}6\lambda$, $\nu = 2{\cdot}5$ and $\alpha = 10°$. The arrows give the directions of the grating orders.

conclusion of our investigation. It represents the average value of intensity on 10 random realizations of a lacunary grating with $N = 15$ and $N_s = 13$. The presence of peaks in the direction of grating orders is all the more surprising since the lacunary grating contains two rods only! The explanation of this phenomenon

seems to be simple: even though the grating contains two rods only, these rods must be located at quantified places which ensures a coherence in the direction of grating orders. The average process favours the coherent directions and thus exhibits the peaks. However, it should be borne in mind that multiscattering effects can completely modify the phenomenon: when only two rods remain in the lacunary grating, the field at infinity can take maximum values in directions different from those of the grating orders. Figure 14 shows that, due to the average process, the prediction of the heuristic reasoning holds.

6. Conclusion

From a rigorous theory of scattering from lacunary gratings, we have been able to estimate the limits of validity of three approximate theories neglecting the anisotropy of the field scattered by each rod. Within the range of validity of the most simple approximate theories, the time-consuming calculations on work-stations using the rigorous theory can be replaced by simple approximate formulae using a pocket calculator. The most simple approximate theory allowed us to predict some simple properties of lacunary gratings having small rods. The first one is that, in the directions of the grating orders, the complex amplitude of the scattered field is proportional to the total number of remaining rods, whatever their locations. The second is the equality of the intensities scattered outside the grating orders by two complementary lacunary gratings.

Finally, our numerical results have permitted us to investigate the transition between periodic gratings and lacunary gratings with large lacunary defect ratios. From these calculations, it emerges that a good means for characterizing the lacunary defect ratio is to measure the incoherence factor. Because of the importance of gratings in reduction of Radar Cross Section, an actual measurement of the lacunary defect ratio from experimental measurements in the microwave region would be very interesting.

Acknowledgments

The work described in this paper has been made in the frame of a contract between the 'Laboratoire d'Optique Electromagnétique' and the 'Direction des Recherches Etudes et Techniques' (French Ministry of Defence).

References

[1] Nieto-Vesperinas, M., and Dainty, J. C., 1990, *Scattering in Volumes and Surfaces* (Amsterdam: North-Holland).
[2] Maystre, D., and Dainty, J. C., 1991, *Modern Analysis of Scattering Phenomena* (New York: Adam Hilger).
[3] Sentenac, A., and Greffet, J. J., 1995, *Waves in Random Media*, **5**, 145.
[4] McGurn, A. R., Maradudin, A. A., and Celli, V., 1985, *Phys. Rev.* B, **31**, 4866.
[5] Arya, K., Su, Z. B., and Birman, J. L., 1985, *Phys. Rev. Lett.*, **54**, 1559.
[6] Sheng, P., White, B., Zhang, Z. Q., and Papanicolaou, G., 1990, *Scattering and Localization of Classical Waves in Random Media*, edited by P. Sheng (London: Word Scientific) 563.
[7] Freilikher, V. D., and Gredeskul, S. A., 1992, Progress in Optics XXX, edited by E. Wolf (Elsevier Science Publishers), p. 137.
[8] Maystre, D., and Saillard, M., 1994, *J. opt. Soc. Am.* A, **11**, 680.

[9] SAILLARD, M., 1994, *J. opt. Soc. Am.* A, **11**, 2704.
[10] FELBACQ, D., MAYSTRE, D., and TAYEB, G., 1995, *J. mod. Optics*, **40**, 473.
[11] SAILLARD, M., and MAYSTRE, D., 1993, *J. opt. Soc. Am.* A, **10**, 502.
[12] SAILLARD, M., POPOV, E., TSONEV, L., SCANDELLA, L., and KRUSE, N., 1995, *Appl. Optics*, **34**, 4883.
[13] FELBACQ, D., TAYEB, G., and MAYSTRE, D., 1994, *J. opt. Soc. Am.* A, **11**, 2526.
[14] ABRAMOVITZ, M., and STEGUN, I., 1970, *Handbook of Mathematical Functions* (New York: Dover).
[15] BORN, M., and WOLF, E., 1959, *Principles of Optics* (London: Pergamon Press).